Original Article

Cytogenet Genome Res 122:73–79 (2008)
DOI: 10.1159/000151319

Cytogenetic and Genome Research

Distribution patterns of phosphorylated Thr 3 and Thr 32 of histone H3 in plant mitosis and meiosis

A.D. Caperta[a, b] M. Rosa[a, d] M. Delgado[a, b] R. Karimi[c] D. Demidov[c] W. Viegas[a] A. Houben[c]

[a]Centro Botânica Aplicada à Agricultura, Instituto Superior de Agronomia, Technical University of Lisbon, and [b]Departamento de Ciências Biológicas e Naturais, Universidade Lusófona de Humanidades e Tecnologias, Lisboa (Portugal); [c]Leibniz Institute of Plant Genetics and Crop Plant Research (IPK), Gatersleben (Germany) [d]Gregor Mendel Institute of Molecular Plant Biology, Vienna (Austria)

Accepted in revised form for publication by B. Friebe, 23 May 2008.

Abstract. Cell cycle dependent phosphorylation of conserved N-terminal tail residues of histone H3 has been described in both animal and plant cells. Through cytogenetic approaches using different plant species we show a detailed description of distribution patterns of phosphorylated histone H3 at either threonine 3 or threonine 32 in mitosis and meiosis. In meristematic cells of the large genome species *Secale cereale, Vicia faba* and *Hordeum vulgare* we have found that phosphorylation of both threonine residues begins in prophase, and dephosphorylation occurs in late anaphase. However, in the small genome species *Arabidopsis thaliana* dephosphorylation occurs at anaphase. In the first division of meiosis of species with large genomes phosphorylation of histone H3 at either threonine 3 or threonine 32 is seen first in diakinesis and extends to anaphase I, whereas in the second division these post-translational modifications are visible at metaphase II through anaphase II. While in *A. thaliana* dephosphorylation takes place at anaphase I and II. In all species analysed phosphorylated H3 at either threonine 3 or threonine 32 are distributed along the entire length of chromosomes during mitotic metaphase and metaphase I. In the second meiotic division threonine 3 phosphorylation is restricted to the pericentromeric domain, while phosphorylation of threonine 32 is widespread along chromosome arms of all species analysed.

Chromatin undergoes dramatic structural changes as the nucleus progresses through the cell cycle, from decondensed interphase chromatin to highly condensed metaphase chromatin. In the control of these events the DNA binding histones regulate chromatin structure and gene expression through dynamic post-translational modifications of their N-terminal tails (Wolffe, 1998). For example the cell cycle dependent phosphorylation of histone H3 at serine 10 (H3S10ph) is tightly correlated with chromosome condensation and segregation (Gurtley et al., 1975; Wei and Allis, 1998). Although Ser 10 phosphorylation and most post-translational modifications of histone H3 are highly conserved, a number of significant differences exist between animals and plants (Fuchs et al., 2006; Houben et al., 2007a). In animals Ser 10 and Ser 28 phosphorylation of histone H3 starts in late G2 in the pericentromeric region from where it is distributed homogeneously throughout the chromosomes (Hendzel et al., 1997; Goto et al., 1999, 2002). In plants, H3 phosphorylation levels at both serine positions are high in pericentromeric regions but very low along the chromosome arms (Houben et al., 1999; Kaszas and Cande, 2000; Manzanero et al., 2000; Pedrosa et al., 2001; Gernand et al., 2003; Schroeder-Reiter et al., 2003). The distribution

Research in the W.V. laboratory was supported by Fundação para a Ciência e Tecnologia, Portugal grant SFRH/BPD/26442 to A.D.C. and SFRH/BPD/27219/2006 to M.D., respectively. D.D., R.K. and A.H. were supported by the Deutsche Forschungsgemeinschaft and by the Land Sachsen Anhalt.

Request reprints from Ana D. Caperta
Centro Botânica Aplicada à Agricultura
Instituto Superior de Agronomia, Technical University of Lisbon
1349-017 Lisboa (Portugal)
e-mail: anadelaunay@isa.utl.pt

1424–8581/08/1221–0073$24.50/0

Accessible online at:
www.karger.com/cgr

of H3S10ph and H3S28ph varies between the two meiotic divisions in plants (Manzanero et al., 2000; Gernand et al., 2003). In the first division, the entire chromosomes are highly phosphorylated, while in the second division H3 phosphorylation is restricted to the pericentromeric regions, similar to mitotic chromosomes. At the same time single chromatids, resulting from equational division of univalents at anaphase I, show low levels of phosphorylation at second meiotic division, suggesting a role of this post-translational modification in sister chromatid cohesion (Manzanero et al., 2000; Gernand et al., 2003).

Phosphorylation of H3 at either Thr 11 (H3T11ph) or Thr 3 (H3T3ph) are spatially distinct from the modifications at Ser 10 and Ser 28 in that both threonine modifications are largely restricted to centromeric regions of condensed mitotic chromosomes in animals (Preuss et al., 2003; Dai et al., 2005). In contrast to animals phosphorylated Thr 11 in plants is distributed along the entire length of condensed chromosomes (Houben et al., 2005). Phosphorylation at Thr 32 (H3T32ph) also occurs in animal cells (Tamada et al., 2006) but the distribution pattern in mitosis and meiosis has not yet been described in either animals or plants.

In the present study we establish a detailed description of distribution patterns of histone H3 phosphorylated at Thr 3 or Thr 32 in mitosis and meiosis of different plant species. The study supports the hypothesis of differential functions of these post-translational modifications in chromosome biology.

Materials and methods

Plant material

The following plant species have been used: *Arabidopsis thaliana* ecotype No-0, *Secale cereale* (rye), *Vicia faba* (field bean) and *Hordeum vulgare* (barley).

Chromosome preparation and indirect immunofluorescence

For immunodetection root tips from all species and selected anthers from *S. cereale* and flower buds from *A. thaliana* were isolated and fixed in 4% paraformaldehyde in phosphate buffered saline (PBS) as previously described (Manzanero et al., 2000). *S. cereale, H. vulgare* and *Vicia faba* root tips were digested with 2% cellulose, 2% cellulase 'Onozuka R-10' and 2% pectinase (Caperta et al., 2002), and squashes were made in PBS. *A. thaliana* flower buds were digested 75 min with 3% cytohelicase, 3% pectolyase and 3% cellulase in PBS at 37°C and squashes were made in PBS. To avoid non-specific antibody binding, slides were blocked for 30 min in 4% (w/v) bovine serum albumin (BSA) plus 0.1% Triton X-100 in PBS at room temperature and incubated with the primary antibodies in a humid chamber. Polyclonal affinity purified rabbit antibodies against H3 phosphorylated at threonine 3 (H3T3ph, Upstate 07-424) and H3 phosphorylated at threonine 32 (H3T32ph, Abcam ab4076) were diluted 1:200 and 1:300 in PBS with 3% BSA respectively. The rat monoclonal antibody against H3 phosphorylated at serine 28 (H3S28ph) (Goto et al., 1999) was diluted 1:400 in PBS with 3% BSA. After 12 h incubation at 4°C and washing for 15 min in PBS, the slides were incubated in rhodamine-conjugated anti-rabbit IgG (Dianova) and FITC-conjugated anti-rat IgG (Dianova) diluted 1:200 in PBS, 3% BSA for 1 h at 37°C. After final washes in PBS, the preparations were counterstained with 4′,6-diamidino-2-phenylindole hydrochloride (DAPI) in Citifluor antifade buffer (AF1; Agar Scientific, Stansted, U.K.).

Fluorescence in situ hybridization (FISH)

A. thaliana preparations were immunodetected as described above and then post-fixed in 4% formaldehyde in PBS followed by FISH. The DNA probe used for FISH analyses was the 180-bp *A. thaliana*-specific centromeric repeat (Copenhaver et al., 1999) labelled with digoxigenin-dUTP by PCR with the primers 5′-ATCCTCTAGAGTCGACCTGCA-3′ and 5′-TTCCCAGTCACGACGTTGTAA-3′, using an initial denaturation step for 4 min at 94°C, and 35 cycles of 94°C for 45 s, 56°C for 45 s, and 72°C for 45 s.

Hybridization conditions, post-hybridization washes and detection of FISH signals were performed according to Pontes et al. (2003). Nuclei were counterstained with DAPI.

Image processing

Analysis of fluorescence signals was recorded with an Olympus BX61 microscope equipped with an ORCA-ER CCD camera (Hamamatsu). Deconvolution microscopy was employed for superior optical resolution of globular structures. Photographs were collected as sequential images along the Z-axis with approximately 11 slices per specimen. Images were collected in grey scale and pseudocolored with Adobe Photoshop, and projections (maximum intensity) were done with the program AnalySIS (Soft Imaging System).

Plant protein extraction

Plant material (200 to 300 mg) was ground under liquid nitrogen and suspended in 1 ml of solubilization buffer (56 mM Na_2CO_3, 56 mM DTT, 2% SDS, 12% sucrose, and 2 mM EDTA). After 10 min of incubation at 70°C, cell debris was removed by centrifugation. 40 μg of protein of each sample were analyzed by protein gel blotting.

For the application of the anti-H3T3ph antibody histone-enriched protein extracts for the analysis were prepared as described by Moehs et al. (1988).

PAGE and protein gel blot analysis

Protein samples were separated by SDS-PAGE in 12% polyacrylamide gels according to Schagger and von Jagow (1987) and then electrotransferred onto polyvinylidene difluoride (PVDF) membranes. After blotting, membranes were reversibly stained with 1% ponceau red. Membranes were incubated for 12 h at 4°C in PBS and 5% low-fat milk or 2× PBS, 5% BSA, 1% PEG 3500, and 1% PVP 10, containing the appropriate antibody. Secondary antibodies conjugated to horseradish peroxidase were used to reveal immunocomplexes by enhanced chemiluminescence (Pierce, Rockford, IL).

Fig. 1. Distribution of phosphorylated histone H3 at Thr 3 (H3T3ph) and Ser 28 (H3S28ph) in somatic cells (**a–d**) and meiocytes (**e–g**) of *Secale cereale*. DAPI stained chromosomes are blue, H3T3ph-specific signals are red, and H3S28ph signals are green. (**a**) Interphase: no signals of H3T3ph and H3S28ph are detected. (**b**) Prophase: H3T3ph is distributed along the chromosome arms whereas H3S28ph is restricted to pericentromeric domains. (**c**) Metaphase: chromosome arms exhibit punctuated H3T3ph pattern along their entire lengths and Thr 3 hyperphosphorylation at outer pericentromeric domains (arrows), while H3S28ph is detected at pericentromeric domains. (**d**) Anaphase: H3T3ph staining is maintained in chromosome arms and Ser 28 phosphorylation remains restricted to pericentromeric domains. (**e**) Diakinesis/metaphase I transition: bivalent chromosomes are stained along chromosome arms for H3T3ph, while H3S28ph is restricted to pericentromeric domains. (**f**) Metaphase II: intense H3T3ph staining is mostly found at outer pericentromeric location and partially co-localize with phosphorylated Ser 28. (**g**) Anaphase II: distribution pattern of H3T3ph is similar to that of metaphase II chromosomes. Bars = 10 μm.

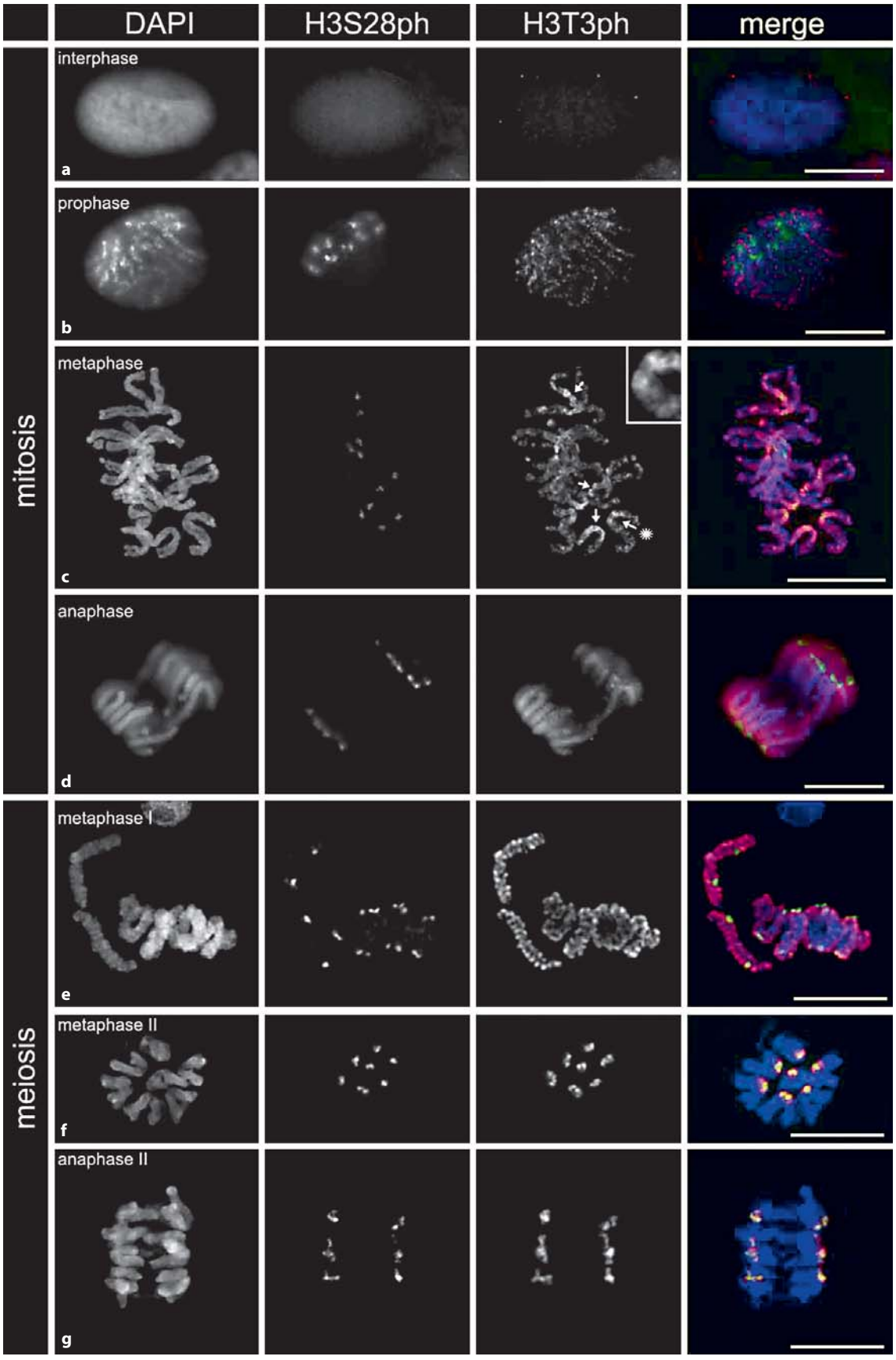
DAPI
H3S28ph
H3T3ph
merge
mitosis
meiosis
interphase
a
prophase
b
metaphase
c
anaphase
d
metaphase I
e
metaphase II
f
anaphase II
g

Results

Different plant species show distinct timings of threonine 3 phosphorylation of histone H3 in somatic cells and meiocytes

The antibodies against phoshorylated histone H3 at either threonine 3 or threonine 32 recognized a protein of the histone H3-type, molecular mass of 17 kDa on Western blots of *A. thaliana* and tobacco protein extracts (supplementary Fig. 1; for online supplementary material, see www.karger.com/doi/10.1159/000151319). The antibodies are likely to recognize the same peptide in plants since the histone H3 amino acid sequences of many plant species are identical to the synthetic peptide sequence used for immunization.

We next determined the chromosomal distribution patterns of histone H3 phosphorylated at threonine 3 (H3T3ph) in mitotic cells of different mono- and dicot species such as *Secale cereale, Hordeum vulgare, Vicia faba* and *A. thaliana*. In all plant species analysed no labelling of interphase chromatin was detected (Fig. 1a; suppl. Fig. 2c). The first immunosignals were detected at prophase, as chromosomes started to condense (Figs. 1b, 2a). In *S. cereale* prophase chromosomes we observed a punctuated dispersed staining along chromosome arms (Fig. 1b). However, a marked difference is observed between different species where phosphorylation of threonine 3 started in early prophase in *A. thaliana*. Sequential immunostaining for H3T3ph and FISH using the *A. thaliana*-specific centromeric 180 bp-repeat as probe revealed that H3T3 phosphorylation starts in close proximity to the centromere. When pericentromeric/centromeric domains of sister chromatids are individualized and seen as FISH-positive double dots, H3T3ph is detected in the regions between the two sister chromatids (Fig. 2a, arrow). In late prophase stage, H3T3ph labelling is dispersed along chromosome arms (Fig. 2b). In all species analysed chromosomes showed an intense phosphorylation labelling when they align to the metaphase plate (Fig. 1c; suppl. Fig. 2a, c). Due to the larger size of *S. cereale* chromosomes we were able to detect a punctuated non-homogeneous phosphorylation staining along chromosome arms and hyperphosphorylation at regions adjacent to centromeric domains (Fig. 1c, arrows, inset). In addition, costaining with antibodies for both H3T3ph and H3S28ph in *S. cereale* revealed that phosphorylated Thr 3 was localized at outer pericentromeric domains while phosphorylated Ser 28 was strongest at inner pericentromeric domains (Fig. 1). Except for *A. thaliana,* where phosphorylation of H3T3 was absent during anaphase (Fig. 2c), in all other species analysed the immunolabelling was maintained until early anaphase (Fig. 1d; suppl. Fig. 2b, d), declined substantially in late anaphase and was absent on decondensing chromosomes at telophase.

In meiosis, phosphorylation of H3 at Thr 3 was initiated during a late step of chromosome condensation, at the transition between diakinesis/metaphase I where chromosomes showed an intense immunolabelling all over the bivalent chromosomes, except for centromeric chromatin (Figs. 1e, 2d). As in mitosis, *S. cereale* bivalents presented strong punctuated labelling until metaphase I (Fig. 1e). In *S. cereale* the immunostaining persisted until late anaphase I and disappeared at telophase I, while in *A. thaliana* meiocytes no Thr3 phosphorylation was detected at anaphase I or telophase I (Fig. 2e). At the second metaphase H3T3ph pattern is similar in both *S. cereale* and *A. thaliana*. The H3T3ph staining is restricted to the regions adjacent to all centromeric domains and no phosphorylation was detected in chromosome arms. This contrasted with the distribution patterns of H3T3ph observed for both metaphase I and metaphase mitotic chromosomes. In *S. cereale,* comparison of H3T3ph distribution with that of H3S28ph at metaphase II revealed partial colocalization of both histone modifications, although H3S28ph labelling is found at the inner position of pericentromeric domains (Fig. 1f). Also *A. thaliana* metaphase II meiocytes (Fig. 2f) presented an H3T3ph distribution pattern similar to that observed for early mitotic prophase (Fig. 2a). Sequential in situ hybridization using the *Arabidopsis* centromeric repeat and immunostaining with the H3T3ph antibody showed minor superimposition between signals. Therefore, metaphase II chromosomes of large and small genomes present a distinct specific distribution pattern in relation to those for mitotic and first meiotic metaphases. In addition, the timings for histone H3 dephosphorylation at threonine 3 at both anaphase I and anaphase II differed between these species, since in *A. thaliana* no labelling is found at this stage, whereas it was still present in *S. cereale*.

A dynamic cell cycle dependent distribution of phosphorylated histone H3 at threonine 32

Next we investigated the cell cycle dependent distribution patterns of phosphorylated threonine 32 of histone H3 in both *A. thaliana* and *S. cereale*. In both species phosphorylation of Thr 32 in somatic cells took place at prophase (Fig. 3a, d) and persisted through metaphase (Fig. 3b, e). In *S. cereale* dephosphorylation occurs at late anaphase, whereas in *A. thaliana* the immunolabelling was absent as early as anaphase (not shown).

In both species we found that histone H3 phosphorylated at threonine 32 is distributed throughout the entire lengths of somatic chromosomes (Fig. 3a, b, d, e). At meiosis, in the

Fig. 2. Distribution pattern of Thr 3 phosphorylation of histone H3 (H3T3ph) in mitotic (**a–c**) and meiotic cells of *A. thaliana* (**d–f**). DAPI stained chromosomes are blue, H3T3ph-specific signals are red, and the FISH signals corresponding to the *A. thaliana* 180-bp centromeric repeat are green. (**a**) Early prophase stage: the immunosignals (red) are adjacent to FISH signals (green). When centromeric domains of sister chromatids are visualized as individual, H3T3ph dots are located intercalary to the centromeric domains in each sister chromatid (arrows). No superimposition between signals is observed. (**b**) Late prophase stage: H3T3ph is dispersed along the chromosome arms and superimposes with centromeric FISH signal. (**c**) Anaphase: no H3T3ph labelling is seen, whereas the FISH signals are detected. (**d**) Diakinesis: phosphorylation is initiated all over entire chromosome lengths except for the pericentromeric regions. (**e**) Anaphase I: no phosphorylation of Thr3 is observed. (**f**) Metaphase II: Thr 3 phosphorylation is detected only in a discrete region between pericentromeric repeats of sister chromatids. Bars = 10 μm.

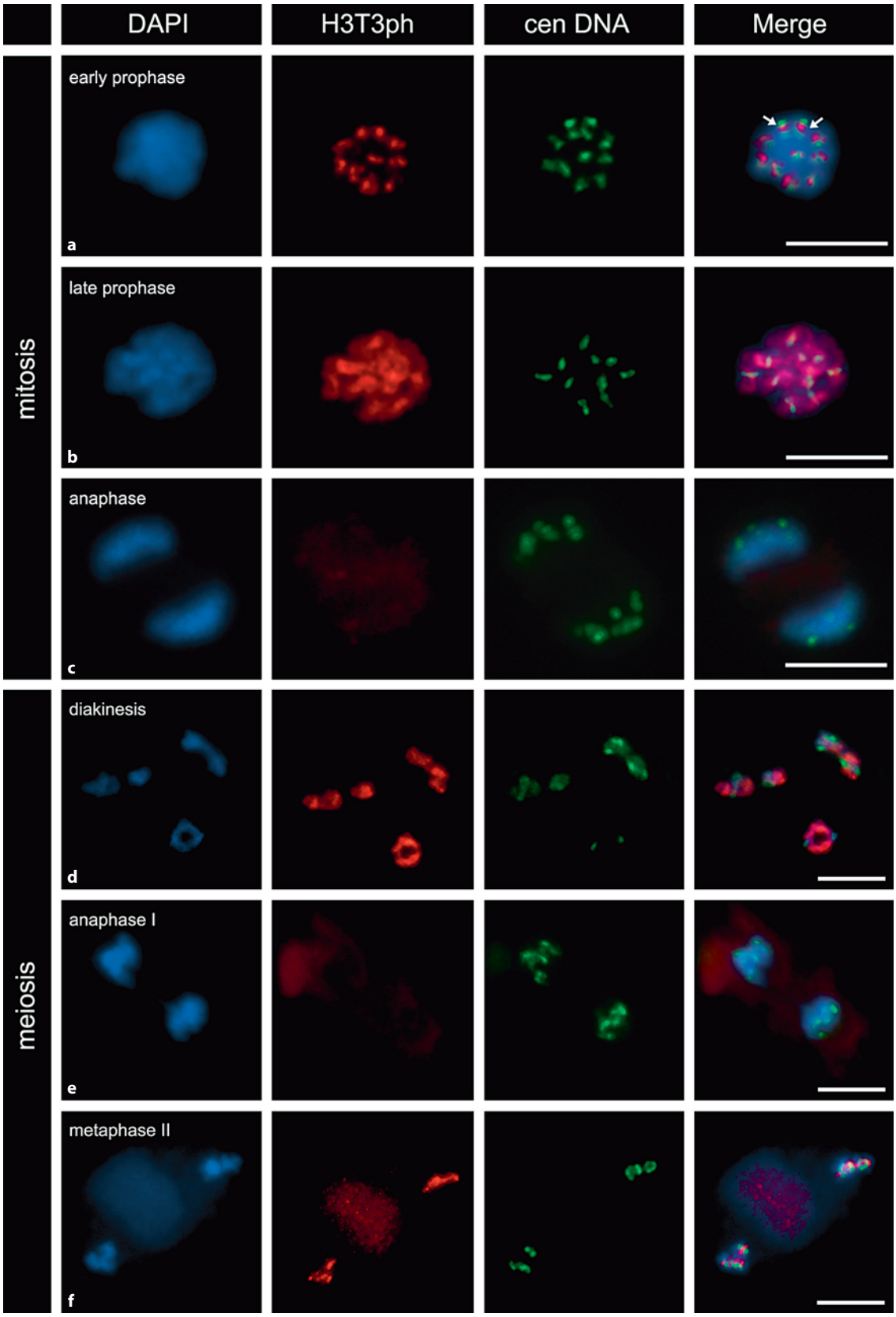
DAPI
H3T3ph
cen DNA
Merge
mitosis
meiosis
early prophase
a
late prophase
b
anaphase
c
diakinesis
d
anaphase I
e
metaphase II
f

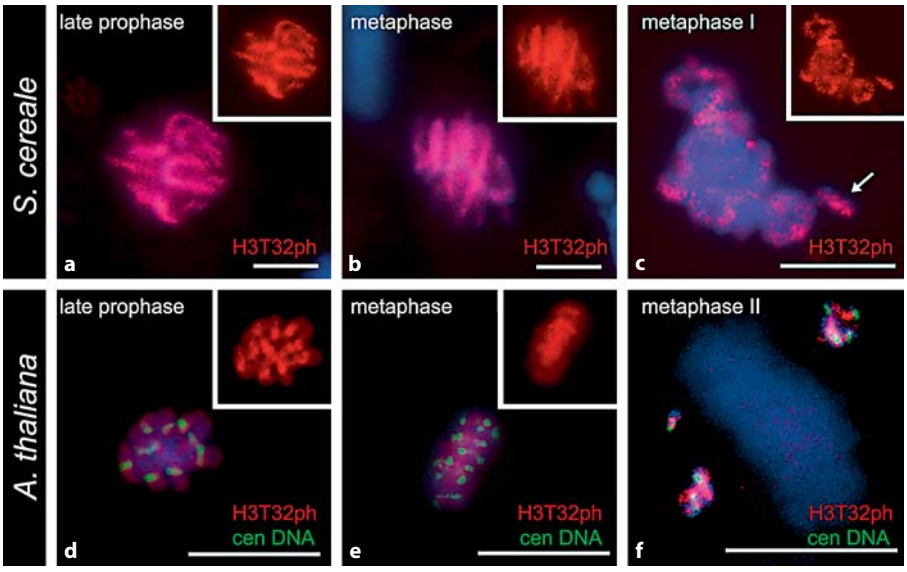

Fig. 3. Thr 32 phosphorylation of histone H3 (H3T32ph) correlates with mitotic and meiotic condensation in *A. thaliana* an *S. cereale*. DAPI stained chromosomes are blue, H3T32ph-signals are red, and the FISH signals corresponding to the *A. thaliana* 180-bp centromeric repeat are green, inset shows H3T32ph signal only. (**a**, **d**) At late prophase H3T32ph-signals coincide with entire lengths of chromosomes and the same is observed at metaphase. (**c**) In diakinesis phosphorylated Thr 32 is dispersed along bivalent arms. B chromosomes are also stained (arrow). (**f**) In the second metaphase of meiosis, the immunosignals are spread along chromosome arms. Bars = 10 μm.

early steps of chromatin condensation (leptotene to pachytene) H3T32 phosphorylation is absent, as determined for Thr 3. In both *A. thaliana* and *S. cereale,* Thr 32 phosphorylation is initiated at diakinesis, and all bivalent chromosomes were immunolabelled along their entire lengths including the supernumerary B chromosomes (Fig. 3c), and went through metaphase I. The immunostaining disappeared at anaphase I and reappeared at metaphase II (Fig. 3f) however, and contrasting with the observations of H3T3ph the entire chromosome arms were labelled at metaphase II.

Discussion

Although the components of the chromatin code are fairly well conserved throughout eukaryotes, evidence is growing that the interpretation of the code has diverged in different organisms, particularly in plants versus animals. Our study provides evidence that in addition to the chromosomal patterns of histone methylation (Houben et al., 2003; Fuchs et al., 2006) phosphorylation of histone H3 also partially varies between species.

Phosphorylation of histone H3 in meristematic cells and meiocytes was followed by the use of polyclonal antibodies that recognize the phosphorylated form of Thr 3 and Thr 32. The detailed distribution patterns of Thr 3 phosphorylation in meiosis, and of Thr 32 phosphorylation in mitosis and meiosis are here described for the first time. For both post-translational modifications we show that the distribution patterns of phosphorylation are correlated with chromosome condensation, although presenting some differences between different species. In mitosis of grasses, the timing of phosphorylation for Thr 3 and Thr 32 begins in prophase, progresses through metaphase when chromosomes are fully compacted, and dephosphorylation occurs at late anaphase, as observed for other phosphorylated residues of histone H3 in plants, i.e. H3S10 (Kaszas and Cande, 2000; Manzanero et al., 2000), H3S28 (Gernand et al., 2003) and H3T11 (Houben et al., 2005). However, in *A. thaliana* dephosphorylation in both residues occurs prior to anaphase. In meiosis both threonine residues are undergoing phosphorylation at diakinesis in a late state of chromosome condensation and progress through metaphase I as it happened for Thr 11 phosphorylation in plants (Houben et al., 2005). The staining of both phosphorylated threonine residues of histone H3 is detected at metaphase II. Again, slight differences in dephosphorylation timing occur between different species. While in the large genome species dephosphorylation is seen at late anaphase I or anaphase II, in *A. thaliana,* it is found during first and second anaphase. Whether the immunostaining pattern differences between the different species are caused by the different genome sizes remains to be tested on a larger number of species.

Additional differences were found between the distribution patterns of H3T3ph and H3T32ph in chromosomes at different cell division stages. In mitotic prophase of *S. cereale* H3T3ph labelling is discontinuous along entire lengths of chromosome arms suggesting a close proximity with heterochromatic domains, namely higher density at the centromeric pole. While in *A. thaliana* phosphorylation at Thr 3 and Thr 32 begins adjacent to the major centromeric heterochromatic domain, and spreads along the chromosome arms in late prophase, when higher chromatin condensation occurs. Also in *A. thaliana* at early prophase some chromosomes show split signals for centromeric DNA with H3T3ph staining in a central location (between sister chromatids), a conformation present in metaphase II chromosomes. A comparable behaviour of centromeric regions was also reported for *Arabidopsis* polyploids at meiosis (Comai et al., 2003). Although those configurations are not yet fully understood, the cruciform organization of pericentric chromatin recently observed in budding yeast represents a good model to explain intramolecular loops adopted by centromere flanking DNA sequences (Yeh et al., 2008).

In metaphase chromosomes of *S. cereale* Thr 3 phosphorylation presents a punctuated distribution pattern along entire lengths of chromosome arms and the pericentromeric domains are hyperphosphorylated, as found for phosphorylated Thr 11 of H3 in plants (Houben et al., 2005). Nevertheless, absence of immunolabelling is observed in centromeric domains in both species. In fact, the signal gap colocalizing with the centromeres may be related to the presence of CENH3 at these regions where no phosphorylation of H3 at Ser 10 has been described in plants (Schroeder-Reiter et al., 2003; Houben et al., 2007b). Collectively, these results contrast with studies in mammalian cells on mitotic chromosomes where the cell cycle dependent phosphorylation at threonines 3 and 11 are restricted to the centromeric regions (Preuss et al., 2003; Dai et al., 2005). Moreover, there are also differences in distribution patterns between the two division phases of meiosis for both H3T3ph and H3T32ph in plants. At diakinesis, the staining spreads uniformly all over the bivalent chromosomes except for the centromeric regions. In mitosis and first meiotic division of species with large genomes, costaining with H3T3ph and H3S28ph antibodies revealed minor superimposition between signals. A similar pattern was detected in metaphase II chromosomes which show hyperphosphorylation of Thr 3 adjacent to phosphorylated serine 28 at the pericentromeric regions and its absence along chromosome arms. These results contrast with patterns here observed for H3T32ph and described for H3T11ph (Houben et al., 2005) which present a uniform distribution along the entire length of condensed chromosomes. Although phosphorylated threonine residues of histone H3 have been associated with chromatin condensation at mitosis and meiosis I, this different phosphorylation dynamics of threonines 3 and 11 at metaphase II stage suggest possible different roles for these post-translational modifications.

Acknowledgements

We thank Augusta Barão and Katrin Kumke for excellent technical assistance. The antibody against H3 phosphorylated at serine 28 was kindly provided by Dr. M. Inagaki.

References

Caperta A, Neves N, Morais-Cecílio L, Malhó R, Viegas W: Genome restructuring in rye affects the expression, organization and disposition of homologous rDNA loci. J Cell Sci 115:2839–2846 (2002).

Comai L, Tyagi A, Lysak M: FISH analysis of meiosis in *Arabidopsis* allopolyploids. Chromosome Res 11:217–226 (2003).

Copenhaver GP, Nickel K, Kuromori T, Benito MI, Kaul S, et al: Genetic definition and sequence analysis of *Arabidopsis* centromeres. Science 286:2468–2474 (1999).

Dai J, Sultan S, Taylor S, Higgins JMG: The kinase haspin is required for mitotic histone H3 Thr 3 phosphorylation and normal metaphase chromosome alignment. Genes Dev 19:472–488 (2005).

Demidov D, Van Damme D, Geelen D, Blattner FR, Houben A: Identification and dynamics of two classes of aurora-like kinases in *Arabidopsis* and other plants. Plant Cell 17:836–848 (2005).

Fuchs J, Demidov D, Houben A, Schubert I: Chromosomal histone modification patterns – from conservation to diversity. Trends Plant Sci 11: 199–208 (2006).

Gernand D, Demidov D, Houben A: The temporal and spatial pattern of histone H3 phosphorylation at serine 28 and serine 10 is similar in plants but differs between mono- and polycentric chromosomes. Cytogenet Genome Res 101: 172–176 (2003).

Goto H, Tomono Y, Ajiro K, Kosako H, Fujita M, et al: Identification of a novel phosphorylation site on histone H3 coupled with mitotic chromosome condensation. J Biol Chem 274:25543–25549 (1999).

Goto H, Yasui Y, Nigg EA, Inaki M: Aurora B phosphorylates histone H3 at serine 28 with regard to the mitotic chromosome condensation. Genes Cells 7:11–17 (2002).

Gurtley LR, Walters RA, Tobey RA: Sequential phosphorylation of histone subfractions in the Chinese hamster cell cycle. J Biol Chem 250: 3936–3944 (1975).

Hendzel MJ, Wei Y, Mancini A, Van Hooser A, Ranalli T, et al: Mitosis-specific phosphorylation of histone H3 initiates primarily within pericentromeric heterochromatin during G2 and spreads in an ordered fashion coincident with mitotic chromosome condensation. Chromosoma 106:348–360 (1997).

Houben A, Wako T, Furushima-Shimogawara R, Presting G, Kunzel G, et al: The cell cycle dependent phosphorylation of histone H3 is correlated with the condensation of plant mitotic chromosomes. Plant J 18:675–679 (1999).

Houben A, Demidov D, Gernand D, Meister A, Leach CR, Schubert I: Methylation of histone H3 in euchromatin of plant chromosomes depends on basic nuclear DNA content. Plant J 33: 967–973 (2003).

Houben A, Demidov D, Rutten T, Scheidtmann KH: Novel phosphorylation of histone H3 at threonine 11 that temporally correlates with condensation of mitotic and meiotic chromosomes in plant cells. Cytogenet Genome Res 109:148–155 (2005).

Houben A, Demidov D, Caperta AD, Karimi R, Agueci F, Vlasenko L: Phosphorylation of histone H3 in plants – a dynamic affair. Biochim Biophys Acta 1769:308–315 (2007a).

Houben A, Schroeder-Reiter E, Nagaki K, Nasud S, Wanner G, et al: CENH3 interacts with the centromeric retrotransposon cereba and GC-rich satellites and locates to centromeric substructures in barley. Chromosoma 116:275–283 (2007b).

Kaszás E, Cande WZ: Phosphorylation of histone H3 is correlated with changes in the maintenance of sister chromatid cohesion during meiosis in maize, rather than the condensation of the chromatin. J Cell Sci 113:3217–3226 (2000).

Manzanero S, Arana P, Puertas MJ, Houben A: The chromosomal distribution of phosphorylated histone H3 differs between plants and animals at meiosis. Chromosoma 109:308–317 (2000).

Moehs C, Mcelwain E, Spiker S: Chromosomal proteins of *Arabidospis thaliana*. Plant Mol Biol 11: 507–515 (1988).

Pedrosa A, Jantsch MF, Moscone EA, Ambros PF, Schweizer D: Characterisation of pericentromeric and sticky intercalary heterochromatin in *Ornithogalum longibracteatum* (Hyacinthaceae). Chromosoma 110:203–213 (2001).

Pontes O, Lawrence RJ, Neves N, Silva M, Lee JH, et al: Natural variation in nucleolar dominance reveals the relationship between nucleolus organizer chromatin topology and rRNA gene transcription in *Arabidopsis*. Proc Natl Acad Sci USA 100:11418–11423 (2003).

Preuss U, Landsberg G, Scheidtmann KH: Novel mitosis-specific phosphorylation of histone H3 at Thr11 mediated by Dlk/ZIP kinase. Nucleic Acids Res 31:878–885 (2003).

Schagger H, von Jagow G: Tricine-sodium dodecyl sulfate-polyacrylamide gel electrophoresis for the separation of proteins in the range from 1 to 100 kDa. Anal Biochem 166:368–379 (1987).

Schroeder-Reiter E, Houben A, Wanner G: Immunogold labeling of chromosomes for scanning electron microscopy: a closer look at phosphorylated histone H3 in mitotic metaphase chromosomes of *Hordeum vulgare*. Chromosome Res 11:585–596 (2003).

Tamada H, Thuan NV, Reed P, Nelson D, Katoku-Kikyo N, et al: Chromatin decondensation and nuclear reprogramming by nucleoplasmin. Mol Cell Biol 26:1259–1271 (2006).

Wei Y, Allis CD: A new marker for mitosis. Trends Cell Biol 8:266 (1998).

Wolffe A: Chromatin Structure and Function, pp 447 (Academic Press, San Diego 1998).

Yeh E, Haase J, Paliulis LV, Joglekar A, Bond L, et al: Pericentric chromatin is organized into an intramolecular loop in mitosis. Curr Biol 18: 81–90 (2008).